

# Selectivity of Protein Interactions Stimulated by Terahertz Signals

Hadeel Elayan, Andrew W. Eckford, and Raviraj Adve

**Abstract**—It has been established that Terahertz (THz) band signals can interact with biomolecules through resonant modes. Specifically, of interest here, protein activation. Our research goal is to show how directing the mechanical signaling inside protein molecules using THz signals can control changes in their structure and activate associated biochemical and biomechanical events. To establish that, we formulate a selectivity metric that quantifies the system performance and captures the capability of the nanoantenna to induce a conformational change in the desired protein molecule/population. The metric provides a score between  $-1$  and  $1$  that indicates the degree of control we have over the system to achieve targeted protein interactions. To develop the selectivity measure, we first use the Langevin stochastic equation driven by an external force to model the protein behavior. We then determine the probability of protein folding by computing the steady-state energy of the driven protein and then generalize our model to account for protein populations. Our numerical analysis results indicate that a maximum selectivity score is attained when only the targeted population experiences a folding behavior due to the impinging THz signal. From the achieved selectivity values, we conclude that the system response not only depends on the resonant frequency but also on the system controlling parameters namely, the nanoantenna force, the damping constant, and the abundance of each protein population. The presented work sheds light on the potential associated with the electromagnetic-based control of protein networks, which could lead to a plethora of applications in the medical field ranging from bio-sensing to targeted therapy.

**Index Terms**—Terahertz, protein interactions, signaling, selectivity, bio-sensing, targeted therapy.

## I. INTRODUCTION

The engineering community is witnessing a new frontier in the communication industry. A network infrastructure consisting of nanodevices is envisioned to enable robust, reliable, and coordinated data transmission. This will also allow for myriad applications in several research fields, including bioengineering, wireless communication, nanotechnology, and environmental sciences. Amongst others, in-vivo wireless nanosensor networks have been presented to provide fast and accurate disease diagnosis and treatment. These networks are capable of operating inside the human body in real-time and will be

We would like to acknowledge the support of the National Science and Engineering Research Council, Canada, through its Discovery Grant program.

H. Elayan and R. Adve are with the Edward S. Rogers Department of Electrical and Computer Engineering, University of Toronto, Ontario, Canada, M5S 3G4 (e-mail: hadeel.mohammad@mail.utoronto.ca; rsadve@ece.utoronto.ca).

A. Eckford is with the Department of Electrical Engineering and Computer Science, York University, Ontario, Canada, M3J 1P3 (e-mail: aeckford@yorku.ca).

of great benefit for medical monitoring and medical implant communication [1].

Researchers have proposed various solutions to realize nanoscale communication, considering both molecular and electromagnetic (EM) communication paradigms. From an EM perspective, plasmonic nano-lasers, plasmonic nano-antennas as well as single-photon detectors all point to the Terahertz (THz) band, defined between 0.1 and 10 THz, as a key enabler of communication at the nanoscale. Numerical analysis and characterization of THz propagation through various body tissues have been presented in [2], [3]. A model that captures intra-body signal degradation is developed in [4]. A multi-layer system that accounts for the discrepancies of human tissues for nano-biosensing applications can be found in [5]. Starting from these works, the importance of studying intra-body nanonetworks has emerged.

THz vibrations are inherently involved in the functionality of biological systems since the energy scale of THz radiation is within the range of interactions between molecules [6]. This overlap in energy bands justifies the particular sensitivity of emerging THz techniques to the molecular motions that underlie intricate biological mechanisms. Specifically, proteins are versatile macromolecules that are responsible for nearly all tasks in a cell. A critical function of proteins is their activity as enzymes, which are needed to catalyze almost all biological reactions. Regulation of the enzyme activity plays a key role in governing the cell behavior. One important feature associated with the protein structure is that it exhibits vibrational spectral features in the THz regime, corresponding to functionally relevant modes. These modes are regarded as the dynamics leading to conformational changes and biomolecular functions [7].

Protein mechanical vibrations can be dipole active, and thus probed using THz dielectric spectroscopy [8]. The extensive review in [7] explores measurements of the THz dielectric response on molecules. The author explains the contributions of the vibrational modes in providing possible information about protein conformational changes, ligand binding and oxidation state. Additionally, the authors in [9] and [10] investigated the mechanical vibrations of the protein lysozyme and the sodium-potassium protein membrane, respectively. Modal analysis was carried out by solving a multi-degree-of-freedom vibration problem and the results were experimentally verified using Raman spectroscopy. The authors indicated a correlation between the resonant peaks found from experiments and the corresponding vibration modes given by numerical simulations.

Further, in a previous work, we proposed a stimulative-responsive paradigm which integrates EM and molecular com-

munication by stimulating proteins in the human body. We analytically derived the mutual information and computed the capacity under different constraints for a two-state [11] and a multi-state protein model [12]. Nonetheless, a fundamental aspect that still must be studied involves understanding the relation between the protein mechanical system and its statistical behavior. This entails being capable of determining the degree of control over the nanoantenna-protein interaction in inducing the desired functional conformational change.

In this work, we develop a theoretical framework to demonstrate the relationship between the protein's mechanical system and the probability of protein folding. We exploit the protein dynamics using the Langevin stochastic equation exposed to an external force, where the protein molecule is modeled as a harmonic oscillator. The Langevin equation is used to capture the components of biological systems, which are constantly subject to random Brownian motion [13]. Since the aim is to model the impact of the nanoantenna on the protein states, we compute the steady-state energy of the induced protein motion and use it to obtain the corresponding Boltzmann's distribution. Our system is generalized to account for a protein population using a normal approximation to the binomial distribution.

Furthermore, we formulate a selectivity metric for both single and multiple proteins to serve as an indicator that quantifies the system performance. The metric provides a score which captures the capability of the nanoantenna to stimulate a conformational change in the desired protein molecule/population without provoking other untargeted proteins in the system to fold. The selectivity values range between  $-1$  and  $1$ . A value of  $-1$  indicates the worst-case scenario, where only the undesired protein molecule/population is being provoked to fold. On the contrary, a value of  $1$  indicates the best-case scenario, where only the desired protein molecule/population is being stimulated to fold. As such, the closer the value achieved to is  $1$ , the higher the selectivity in the system. Finally, a value of  $0$  reflects either the case where neither the desired nor the undesired proteins experience a conformational change or the case where both the desired and undesired proteins experience conformational changes. Both aforementioned scenarios indicate that the system is being non-selective since selectivity demands only the desired protein molecule/population to experience folding. From this perspective, we make the following contributions:

- We formulate an expression for the induced protein steady-state energy due to THz radiation. The energy expression links the mechanical system of the protein to the probability of protein folding.
- We generalize our system to account for a protein population. We then present a selectivity metric to serve as a tool that determines the capability of THz nanosensors in governing protein interactions in an intra-body network.
- We formulate a joint optimization problem to retrieve the optimal nanoantenna force and frequency values that maximize the selectivity.

The rest of the paper is organized as follows. In Sec. II, we present the system model of the driven protein dynamics.

In Sec. III, we formulate the expression of the steady-state energy driving the protein to change its conformation and use it to modify Boltzmann distribution. In Sec. IV, we formulate a metric to account for the selectivity of the nanoantenna-protein interaction. In Sec. V, we demonstrate our numerical results based on the developed model. Finally, we draw our conclusions in Sec. VI.

## II. SYSTEM MODEL

### A. Physical Basis

Our system is composed of a nanoantenna transmitter and a protein receiver. Plasmonic nanoantennas can provide both enhanced and controllable EM-matter interactions in addition to strong coupling between far-field radiation and localized sources at the nanoscale [14]. These nanoantennas with typical dimensions on the order of a few hundred nanometers have found their applications in bio-sensing, bio-imaging, as well as energy harvesting. In this manuscript, our nanoantenna operates in the THz frequency range [15], [16].

THz plasmonic waves have propagation distances of hundreds or thousands of wavelengths, whereas plasmonics at higher frequencies typically have propagation lengths of only a few tens of wavelengths [17]. To read more about THz plasmonic waves, we direct interested readers to this review article [18]. It is to be noted that in our current work, we consider a dipole nanoantenna designed for the incident frequency being used, which is tuned to the vibrational frequency of the desired protein, without considering the specifics of the antenna.

The transmission from the nanoantenna impinges EM waves on the protein population to target distinct vibrational modes and trigger a functional conformational change. Application of an external EM field to biological entities induces a relative redistribution of internal charges within the molecule with respect to the field lines [19]. This results in a dielectric response that is frequency dependent. Subsequently, the nanoantenna EM field leads to the polarization of the protein molecule. By examining the protein dielectric response, dynamical transitions in the protein structure at the THz frequency range can be attributed to relaxational and resonant processes. Relaxational responses arise from the amino acid side chains, while resonant responses stem from the correlated motions of the protein structure [20]. Correlated motion occurs when many parts of the system are coupled and oscillate simultaneously. This suggests the capability of tuning the nanoantenna to the vibrational frequency of the protein to provoke desired functional resonant interactions.

The protein permittivity formulated as,  $\varepsilon(\omega) = \varepsilon'(\omega) - j\varepsilon''(\omega)$ , has its real part given by [20]

$$\varepsilon'(\omega) = \varepsilon_\infty + \frac{\varepsilon_0 - \varepsilon_\infty}{1 + (\omega\tau)^2} + \frac{(\varepsilon_1 - \varepsilon_\infty) \left[ 1 - \left( \frac{\omega}{\omega_0} \right)^2 \right]}{\left[ 1 - \left( \frac{\omega}{\omega_0} \right)^2 \right]^2 + (\omega\gamma)^2}, \quad (1)$$

while the imaginary part yields

$$\varepsilon''(\omega) = \frac{(\varepsilon_o - \varepsilon_\infty)\omega\tau}{1 + (\omega\tau)^2} + \frac{(\varepsilon_1 - \varepsilon_\infty)\omega\gamma}{\left[1 - \left(\frac{\omega}{\omega_o}\right)^2\right]^2 + (\omega\gamma)^2}. \quad (2)$$

Here,  $\tau$  is the protein relaxation time,  $\omega_o$  is the natural frequency of the protein, and  $\gamma$  is the damping constant.  $\varepsilon_\infty$  is the permittivity at the high frequency limit,  $\varepsilon_o$  is the relative permittivity at low frequencies (static region) and  $\varepsilon_1$  refers to an intermediate permittivity value. The damping constant  $\gamma$  governs the magnitude of the resonances. In fact, damping forces, which slow the motion of proteins, are due to both solvent and protein friction, where the viscosity arises either from the surrounding fluid or from interactions between amino acids.

According to structural mechanics, if an external harmonic excitation has a frequency which matches one of the natural frequencies of the system, then resonance occurs, and the vibrational amplitude of the structure increases [21]. When two oscillators are in resonance, two important characteristics hold, namely, high energy efficiency and rapidity. This means that nearly all of the energy can be transferred between the elements and that the speed of resonant exchange in energy is fast [22]. As such, a nanoantenna tuned to the resonant frequency of a distinct protein vibrational mode can stimulate protein signaling. By triggering the protein to adopt a folding behavior, a series of downstream events occur within the cell, enabling a functional response.

To study and evaluate the impact of the nanoantenna-protein interaction, we formulate a *selectivity* metric to show the capability of the presented system in discriminating the desired response from adjacent inputs. Particularly, the developed metric measures the capability of the nanoantenna to stimulate the desired protein molecule/population to change its conformation without impacting the conformation of other proteins in the system. Such a metric provides a powerful tool as it gives a single value to quantitatively decide whether or not an interaction is sufficiently controllable.

The selectivity analysis lays the grounds for directed signaling, where desired proteins are driven towards a conformation that evokes a particular response. It also paves the path towards a plethora of applications in the medical field. On the one hand, it allows us to recognize mechanisms for selectively targeting proteins involved in carcinogenesis, a procedure which can be utilized for the early diagnosis of cancer cells. On the other hand, it could further the understanding of neurodegenerative diseases, which are primarily caused due to the aggregation of misfolded proteins. Finally, the presented work has broad implications for improving our understanding of proteins, protein engineering and better drug design.

## B. Mathematical Model

To model the protein dynamics, we use the Langevin stochastic equation under the influence of an external force. The Langevin equation allows us to analyze the forces acting on the protein by virtue of the impacts received from the nanoantenna external force as well as the random forces

originating from the interactions of the surrounding particles. It is given as [23]

$$m \frac{d^2x}{dt^2} + \beta \frac{dx}{dt} + kx(t) = f_{ex}(t) + f_\zeta(t), \quad (3)$$

where  $x = x(t)$  is the protein coordinate,  $m$  is the protein mass,  $k$  is the protein spring constant (stiffness), and  $\beta$  is the damping coefficient. In (3),  $f_{ex}(t) = f_o \cos(\omega t)$  is the external driving nanoantenna force. This force arises from the interaction of the incident electric field of the antenna with the protein, where the protein is treated as a dielectric. Mathematically, the force scales linearly with the gradient squared of the electric field [24].

In addition,  $f_\zeta(t)$  is the stochastic force acting on the protein, which is governed by a white-noise fluctuation-dissipation relation as follows [25]

$$f_\zeta(t) = \sqrt{\Gamma}\zeta(t). \quad (4)$$

$\zeta(t)$  is a white, Gaussian random process with moments [25]

$$\begin{aligned} \langle \zeta(t_1) \rangle &= 0 \\ \langle \zeta(t_1)\zeta(t_2) \rangle &= \delta(t_1 - t_2). \end{aligned} \quad (5)$$

Here,  $\langle \cdot \rangle$  defines the statistical average of a quantity. In (4),  $\Gamma = 2\gamma mk_b T$  denotes the strength of the noise  $\zeta(t)$ . It fixes the amplitude of the fluctuation in the random force in terms of both the temperature and the dissipation coefficient [25]. In addition, (3) can be re-written as

$$\frac{d^2x}{dt^2} + \gamma \frac{dx}{dt} + \omega_o^2 x(t) = \frac{1}{m} [f_{ex}(t) + f_\zeta(t)], \quad (6)$$

where  $\gamma = \beta/m$  and  $\omega_o^2 = k/m$ .

Green's function is a powerful mathematical tool to solve inhomogeneous differential equations. It provides the solution to the inhomogeneous equation with a forcing term given by a point source. For an arbitrary forcing term, the solution to the same equation is formulated by integrating Green's function against the forcing term. The frequency-domain solution of Green's function corresponding to (6) is found as [26]

$$G(\omega, t') = \frac{e^{j\omega t'}}{m[-\omega^2 - j\gamma\omega + \omega_o^2]}. \quad (7)$$

The final form of Green's function is given by [26]

$$G(t, t') = \frac{1}{m\alpha} e^{-\frac{\gamma}{2}(t-t')} \sin[\alpha(t-t')] \Theta(t-t'), \quad (8)$$

where  $\alpha = \sqrt{\omega_o^2 - \frac{\gamma^2}{4}}$  and  $\Theta(t-t')$  denotes the step function

$$\Theta(t-t') = \begin{cases} 1, & \text{for } t \geq t' \\ 0, & \text{otherwise.} \end{cases} \quad (9)$$

In this paper, we will consider  $\omega_o > \frac{\gamma}{2}$ . Physically, this condition satisfies protein collective vibrations, where protein modes in the THz frequency range have been shown to be underdamped even in aqueous solutions [27]–[29].

The solution of (3) can be decomposed into two parts, one related to the deterministic nanoantenna external force  $f_{ex}(t)$  and the other related to the stochastic force  $f_\zeta(t)$ , resulting in  $x(t) = x_{ex}(t) + x_\zeta(t)$ . The solution corresponding to the

nanoantenna force can be expressed using the time-domain Green's function as [30]

$$\begin{aligned} x_{ex}(t) &= \int_0^\infty G(t, t') f_{ex}(t') dt' \\ &= \frac{f_o}{m\alpha} \int_0^t e^{-\frac{\gamma}{2}(t-t')} \sin[\alpha(t-t')] \cos(\omega t') dt' \quad (10) \\ &= A \cos(\omega t - \phi) - A \frac{\omega_o}{\alpha} \cos(\omega t - \phi) e^{-\frac{\gamma}{2}t}, \end{aligned}$$

where

$$A = \frac{f_o}{m\sqrt{(\omega_o^2 - \omega^2)^2 + (\omega\gamma)^2}}, \quad (11)$$

$$\tan \phi = \frac{\gamma\omega}{(\omega_o^2 - \omega^2)}, \quad (12)$$

and

$$\tan \varphi = \frac{\gamma(\omega_o^2 + \omega^2)}{2\alpha(\omega_o^2 - \omega^2)}. \quad (13)$$

Similarly, the solution corresponding to the stochastic component can be expressed as

$$\begin{aligned} x_\zeta(t) &= \int_0^\infty G(t, t') f_\zeta(t') dt' \\ &= \sqrt{\Gamma} \int_0^\infty G(t, t') \zeta(t') dt'. \end{aligned} \quad (14)$$

Here  $x_\zeta(t)$  is a linear function of  $\zeta(t)$ , and therefore is also Gaussian.

### III. BOLTZMANN DISTRIBUTION: RELATING ENERGY TO PROBABILITY

Amino acids are considered the building blocks of protein synthesis. The amino acids that reside in the cytoplasm conduct movements through the rotation of the intracellular churn alongside the molecular interactions upon them. In addition, ATP usage serves as a biological instigator for the interactions of amino acids. Such active and mass consumption of amino acids necessitate the constant flow of high levels of energy, which in absence results in further irreparable harm to cellular functions by disabling the conduction of protein activities [31].

The necessity of energy exchange to trigger a protein conformational change in our system highlights the need for interfacing THz-band signals with protein molecules to initiate resonance. This will allow minuscule bodies to express large amplitude oscillations. To find the total energy of a protein stimulated by an external force in a stochastic environment, we compute both the kinetic and potential energy contributions as follows [32]

$$\langle E_{tot} \rangle_{ss} = \frac{1}{2} m \langle v^2(t) \rangle_{ss} + \frac{1}{2} k \langle x^2(t) \rangle_{ss}. \quad (15)$$

We denote by  $\langle \cdot \rangle_{ss}$  the statistical average value in steady-state, where all transient effects die out. We also use  $\overline{(\cdot)}_{ss}$  to refer to the mean value in steady-state. The only difference between both notations is that one of them comes from a stochastic component, while the other comes from a deterministic component, respectively. To derive (15), we utilize the solution of the Langevin equation derived in Sec. II-B, which is given by  $x_{ex}(t)$  and  $x_\zeta(t)$ .

We first evaluate the potential energy by finding the mean squared displacement of the protein,  $\langle x^2(t) \rangle_{ss}$ , which is decomposed into the contributions of the external force and stochastic force, respectively. It is given as

$$\langle x^2(t) \rangle_{ss} = \overline{(x_{ex}^2(t))}_{ss} + \langle x_\zeta^2(t) \rangle_{ss}. \quad (16)$$

$\langle x^2(t) \rangle_{ss}$  is a measure of the spatial extent of the protein motion. From (10), we compute  $\overline{(x_{ex}^2(t))}_{ss}$ , as

$$\begin{aligned} \overline{(x_{ex}^2(t))}_{ss} &= \overline{\left( A \cos(\omega t - \phi) - A \frac{\omega_o}{\alpha} \cos(\omega t - \phi) e^{-\frac{\gamma}{2}t} \right)^2}_{ss} \\ &= \frac{A^2}{2}. \end{aligned} \quad (17)$$

In addition, to find  $\langle x_\zeta^2(t) \rangle_{ss}$ , we apply Parseval's theorem, where we use the following corollaries

$$\langle x_\zeta^2(t) \rangle_{ss} = \frac{1}{T} \int_{-T/2}^{T/2} \langle |x_\zeta(t)|^2 \rangle dt = \frac{1}{2\pi} \int_{-\infty}^{\infty} \langle |x_\zeta(\omega)|^2 \rangle d\omega. \quad (18)$$

$\langle |x_\zeta(\omega)|^2 \rangle$  is found from (7) using the frequency domain Green's function along with the stochastic force defined in (4) as follows

$$\langle |x_\zeta(\omega)|^2 \rangle = |G(\omega)\sqrt{\Gamma}|^2 = \frac{\Gamma}{m^2 \left[ (\omega_o^2 - \omega^2)^2 + (\omega\gamma)^2 \right]}. \quad (19)$$

From (19), we compute the integration in (18) by using the residue theorem, which evaluates line integrals of analytic functions over closed curves. This results in

$$\begin{aligned} \langle x_\zeta^2(t) \rangle_{ss} &= \frac{1}{2\pi} \int_{-\infty}^{\infty} \langle |x_\zeta(\omega)|^2 \rangle d\omega \\ &= \frac{1}{2\pi} \int_{-\infty}^{\infty} \frac{\Gamma}{m^2 \left[ (\omega_o^2 - \omega^2)^2 + (\omega\gamma)^2 \right]} d\omega \quad (20) \\ &= \frac{\Gamma}{2\pi m^2} \frac{\pi}{\gamma\omega_o^2} = \frac{k_b T}{m\omega_o^2} = \frac{k_b T}{k}. \end{aligned}$$

In a similar manner, to evaluate the kinetic energy, we need to compute  $\langle v^2(t) \rangle_{ss}$  which is given as

$$\langle v^2(t) \rangle_{ss} = \overline{(v_{ex}^2(t))}_{ss} + \langle v_\zeta^2(t) \rangle_{ss}. \quad (21)$$

$\overline{(v_{ex}^2(t))}_{ss}$  is calculated from the derivative of the displacement  $x_{ex}(t)$  given in (10), where we first find  $v_{ex}(t)$  as follows

$$\begin{aligned} v_{ex}(t) &= \dot{x}_{ex}(t) = -\omega A \sin(\omega t - \phi) \\ &\quad + A \frac{\omega_o}{\alpha} e^{-\frac{\gamma}{2}t} \left( \omega \sin(\omega t - \phi) + \frac{\gamma}{2} \cos(\omega t - \phi) \right). \end{aligned} \quad (22)$$

We then compute the mean squared value of (22) which leads to

$$\overline{(v_{ex}^2(t))}_{ss} = \overline{(\dot{x}_{ex}(t))^2}_{ss} = \frac{\omega^2 A^2}{2}. \quad (23)$$

Likewise,  $\langle v_\zeta^2(t) \rangle_{ss}$  is found from the Fourier transform of the derivative of the displacement. From (20), we have

$$\begin{aligned} \langle v_\zeta^2(t) \rangle_{ss} &= \frac{1}{2\pi} \int_{-\infty}^{\infty} \langle |x_\zeta(\omega)|^2 \rangle \omega^2 d\omega \\ &= \frac{\Gamma}{2\pi m^2} \int_{-\infty}^{\infty} \frac{\omega^2}{(\omega_o^2 - \omega^2)^2 + (\omega\gamma)^2} d\omega \\ &= \frac{\gamma k_b T}{\pi m} \frac{\pi}{\gamma} \\ &= \frac{k_b T}{m}. \end{aligned} \quad (24)$$

Finally, we can find the total steady-state energy of the driven protein motion by substituting (16) and (21) in (15) yielding

$$\begin{aligned} \langle E_{\text{tot}} \rangle_{ss} &= \frac{1}{4} m A^2 (\omega^2 + \omega_o^2) + k_b T \\ &= \frac{1}{4} \underbrace{\left[ \frac{f_o^2 (\omega^2 + \omega_o^2)}{m((\omega_o^2 - \omega^2)^2 + (\omega\gamma)^2)} \right]}_{\text{THz Force Contribution}} + \underbrace{k_b T}_{\text{Noise Effect}}. \end{aligned} \quad (25)$$

From (25), we can see that the derived expression reflects the capability of the applied electric field since the energy absorbed is in excess of that of thermal noise, i.e.,  $k_b T$ . Thus, for resonances to have an important effect on biological systems, the effect of the applied field should be greater than the corresponding random field.

Moreover, signaling inside proteins results in a spring-like effect which shifts their energy [33]. Protein structures are therefore investigated using energy functions where they obey statistical laws based on the Boltzmann distribution. Specifically, the Boltzmann distribution provides the probability that a system will be in a certain state as a function of the state's energy and system temperature [34]. In the presented two-state model, the protein resembles a binary biological switch. The states of the protein depicted are folded and unfolded, as those govern the activation of biological processes and chemical interactions. The input to our channel is the force induced by the nanoantenna, while the output is the state of the protein.

The rate of protein folding is given by [35]

$$r_f = r_0 \exp\left(\frac{-E_f}{k_b T}\right), \quad (26)$$

where  $E_f$  denotes the Gibbs free energy generated through metabolic processes and associated with the folded protein state.  $r_0$  is a scale factor that preserves detailed balance. In our case, the rate of protein folding must incorporate the steady-state energy of the driven protein motion,  $\langle E_{\text{tot}} \rangle_{ss}$ , computed in (25) as follows

$$r_f = r_0 \exp\left(\frac{-E_f + \langle E_{\text{tot}} \rangle_{ss}}{k_b T}\right). \quad (27)$$

In addition, the unfolding transition is a relaxation process that returns the protein to the unfolded state. In this view, the unfolded state is actually an equilibrium distribution of many unfolded or partially folded conformational states. Such a process is considered independent of the imposed signal [36] and is given by

$$r_u = r_0 \exp\left(\frac{-E_u}{k_b T}\right), \quad (28)$$

where  $E_u$  denotes the Gibbs free energy associated with the unfolded protein state. Consequently, the rate of change of the protein folding probability is

$$\frac{d}{dt} p_f(t) = -r_u p_f(t) + r_f (1 - p_f(t)), \quad (29)$$

where  $p_f(t)$  is the probability that the protein is in the folded state at time  $t$ . The corresponding probability of the unfolded state is given by  $p_u(t) = 1 - p_f(t)$ . From (29), the stationary solution can be found as

$$p_F = \frac{r_f}{r_f + r_u}. \quad (30)$$

Substituting (27) and (28) in (30) yields

$$p_F = \frac{1}{1 + \exp\left(\frac{\Delta E - \langle E_{\text{tot}} \rangle_{ss}}{k_b T}\right)}, \quad (31)$$

where  $\Delta E = E_f - E_u$ . The values of  $\Delta E$  for different proteins can be found from experimental studies available in the literature since protein folding and unfolding is a naturally occurring phenomenon driven by the change in free energy.

The state of a single protein can be regarded as a Bernoulli random variable with a probability of success,  $p_F$ . As such, when considering a system composed of  $n$  proteins, the random number of folded proteins,  $n_F$ , follows a binomial distribution that is given by

$$p(n_F | p_F) = \binom{n}{n_F} p_F^{n_F} (1 - p_F)^{n - n_F}. \quad (32)$$

In addition, due to the large diversity of proteins seen in an intra-body environment, the binomial distribution can be approximated by a normal distribution with mean,  $\mu = n p_F$ , and variance,  $\sigma^2 = n p_F (1 - p_F)$ , i.e.,

$$n_F \sim \mathcal{N}(n p_F, n p_F (1 - p_F)). \quad (33)$$

We define protein population as the number of copies of a protein molecule in a cell. Hence, the number of folded proteins of each protein population,  $i$ , can be expressed as a normal distribution as follows

$$n_{F,i} \sim \mathcal{N}(n p_{F,i}, n p_{F,i} (1 - p_{F,i})). \quad (34)$$

#### IV. SELECTIVITY OF THE NANOANTENNA-PROTEIN INTERACTION

Folding of proteins into their correct native structure is key to their function, whereas unfolded or misfolded proteins contribute to a pathology of many diseases [37]. When a nanoantenna targets a protein population, it is expected to affect the conformational change in the cytoplasmic domain of the *desired* receptor molecules in order to induce a particular functional response. In other words, a protein interaction must be selective to achieve control over the protein network.

In the context of this work, *selectivity* is introduced as a system performance metric that quantifies the ability of the nanoantenna to provoke a conformational change in the desired protein molecule/population without impacting a similar conformation of other untargeted proteins. A maximum selectivity score is expected when only the targeted population

experiences a folding behavior due to the impinging THz signal. Therefore, the selectivity is an indicator as to whether or not an interaction is sufficiently controllable. The focus on developing a selectivity metric stems from the fact that selectivity is the most important feature that reflects if THz-stimulated interactions can be adequately controlled to enable useful signal transduction processes.

Selectivity arises in the literature in various scenarios. In drug discovery, it refers to the experimenter's ability to design maximally selective ligands that act on specific targets. Poor selectivity in this context may result in toxicity and side effects [38]. Moreover, for ion channels, the selectivity feature arises at permeable membranes, where it allows the passage of some molecules and inhibits the passage of others [39]. Further, selectivity appears as a measure of the performance of a radio receiver when it responds only to the radio signal it is tuned to and rejects other signals nearby in frequency.

In this work, the presented selectivity metric has been formulated after extensively investigating the literature. Our choice of measure relies on the interpretation of the metric in terms of the problem considered, its analytical properties and ease of computation. In fact, it came to our attention that many of the available measures used in other contexts and applications, such as the Bhattacharyya distance, the Chernoff distance, and the Kullback-Leibler divergence, are unbounded from above, and therefore are not suitable for our application since they cannot directly guide experimenters to whether an interaction is selective or not.

To assess the level of control imposed by THz signals over protein interactions, we propose in this work a selectivity metric given by

$$S(p_{F,d}, p_{F,ud}) = \frac{p_{F,d} - p_{F,ud}}{\max(p_{F,d}, p_{F,ud})}, \quad (35)$$

where  $p_{F,d}$  is the probability of the folded state of the desired protein, while  $p_{F,ud}$  is the probability of the folded state of the undesired protein. The denominator involves a max function for normalization purposes. Since the developed metric relies on the stationary probability difference,  $p_{F,d} - p_{F,ud}$ , it captures both the system mechanical parameters and the amount of energy stored in the THz-stimulated protein.

Our developed selectivity metric has a number of properties which renders it as a powerful tool for evaluating protein interactions in the system. Those properties include:

- $S(p_{F,d}, p_{F,ud})$  is bounded, such that  $-1 \leq S(p_{F,d}, p_{F,ud}) \leq 1$ .
- $S(p_{F,d}, p_{F,ud})$  has a **maximum value** of 1 indicating that **both** the targeted protein was selected **and** the untargeted protein was not selected. This occurs when  $p_{F,d} = 1$  and  $p_{F,ud} = 0$ . A value of 1 indicates the best-case scenario.
- $S(p_{F,d}, p_{F,ud})$  has a **minimum value** of -1 indicating that **both** the untargeted protein was selected **and** the targeted protein was not selected. This occurs when  $p_{F,d} = 0$  and  $p_{F,ud} = 1$ . A value of -1 indicates the worst-case scenario.
- $S(p_{F,d}, p_{F,ud})$  is continuous and an increasing function of  $p_{F,d}$  when  $p_{F,ud}$  is fixed.

When dealing with a protein *population*, the selectivity metric can be adjusted based on the separation of the means of the populations. The comparison of two independent population means is a very common tool. It actually provides a way to test whether the two groups differ by capturing the overlap between the protein populations in the system. As such, it can signal whether or not it is possible to target the desired protein population. In this case, the selectivity metric is defined as

$$S(\mu_d, \mu_{ud}) = \frac{\mu_d - \mu_{ud}}{\max(\mu_d, \mu_{ud})}, \quad (36)$$

where  $\mu_d$  and  $\mu_{ud}$  are the means of the desired and undesired protein populations, respectively. The same properties which hold for (35) still holds in (36). In fact, when the population of both the desired and undesired protein categories equal  $n$ , (36) reduces to (35), where  $S(\mu_d, \mu_{ud}) = S(np_{F,d}, np_{F,ud}) = S(p_{F,d}, p_{F,ud})$ .

In addition, an interesting feature of the presented measure is its scalability as it can account for multiple undesired proteins in the system, while still holding its aforementioned properties. For such a case, the selectivity is given by

$$S(\mu_d, \boldsymbol{\mu}_{ud}) = \frac{\mu_d - \sum_i \mu_{ud,i}}{\max(\mu_d, \sum_i \mu_{ud,i})}, \quad (37)$$

where  $\sum_i \mu_{ud,i}$  refers to the sum over all the means of the undesired protein populations in the system.

#### A. Optimal System Design Parameters

In order to trigger a specific protein population to activate the desired system response, we must ensure that the system achieves maximum selectivity. From (25), we can notice that the nanoantenna frequency,  $\omega$ , and the nanoantenna force,  $f_o$ , are the only system parameters that we can control. Thereby, we formulate a joint optimization problem to maximize the selectivity with respect to those parameters. To simplify (35), an intuitive assumption is to only consider the scenario  $p_{F,d} > p_{F,ud}$ . This holds true since we are tuning the nanoantenna to the resonant frequency of the desired protein population. Thus, the selectivity becomes

$$S(p_{F,d}, p_{F,ud}) = \frac{p_{F,d} - p_{F,ud}}{p_{F,d}} = 1 - \frac{p_{F,ud}}{p_{F,d}}. \quad (38)$$

Hence, what we are essentially interested in maximizing is the stationary folding probability ratio of the desired and undesired proteins,  $p_{F,d}/p_{F,ud}$ . The optimization problem is therefore given as

$$\begin{aligned} & \underset{f_o, \omega}{\text{maximize}} && S(p_{F,d}, p_{F,ud}) \\ & \text{subject to} && 0 \leq p_{F,d} \leq 1 \\ & && 0 \leq p_{F,ud} \leq 1. \end{aligned} \quad (39)$$

To solve (39), we use the fixed-point iteration method [40]. Specifically, given a function  $g(x)$  defined on real numbers, and given a point  $x_0$  in the domain of  $g(x)$ , the fixed-point iteration is  $x_{j+1} = g(x_j)$ ,  $j = 0, 1, 2, \dots$ , which gives rise to the sequence  $x_0, x_1, x_2, \dots$ . Under some mild conditions, the sequence converges to the fixed point  $\bar{x}$  [40]. Hence, the values

of the force and frequency that maximize the selectivity are retrieved, as detailed in Algorithm 1. We note that the same procedure is applied to maximize selectivity in the case of protein population.

---

**Algorithm 1** Joint Optimization using Fixed-Point Iteration
 

---

- 1: Initialize the max number of iterations  $I_{max}$  and the allowed error tolerance  $\epsilon$ . Set the iteration index  $k = 0$ . Initialize the force  $f_0$  and the frequency  $\omega_0$
  - 2: **repeat**
  - 3:    $f_{k+1} = g_f(f_k)$  and  $\omega_{k+1} = g_\omega(\omega_k)$
  - 4:   **if**  $|f_{k+1} - f_k| < \epsilon$  and  $|\omega_{k+1} - \omega_k| < \epsilon$ , **then**
  - 5:      $f^* = f_{k+1}$
  - 6:      $\omega^* = \omega_{k+1}$
  - 7:   **else**
  - 8:      $f_k = f_{k+1}$
  - 9:      $\omega_k = \omega_{k+1}$
  - 10:   **end if**
  - 11: **until**  $k = I_{max}$
  - 12: **Output:**  $f^*, \omega^*$
- 

## V. NUMERICAL RESULTS

In this section, we demonstrate the results of numerically simulating our analytical model. For our analysis, we will consider several cases of protein populations in the vicinity of one other to mimic different intra-body scenarios. Those proteins include rhodopsin, bacteriorhodopsin and D96N bacteriorhodopsin. The aforementioned proteins serve as excellent model systems for studying properties of membrane proteins. Nonetheless, although they contain seven  $\alpha$ -helical transmembrane domains, each has a different topology. The description of the normal mode motion and its associated vibrational frequency for each of those proteins has been obtained from [41], while their mechanical properties were found in [42] as summarized in Table I. It is to be noted that although the frequencies we will focus on in the numerical results are those of rhodopsin (1.36 THz) and bacteriorhodopsin (1.13 THz), protein vibrational frequencies span the range between 0.03-6.0 THz [43]. In addition, unless otherwise stated, we consider a protein population of  $n = 1000$ .

### A. Protein Response to Nanoantenna

Fig. 1a presents the expected number of proteins in the folded state,  $E[n_F] = np_F$ , versus the nanoantenna force for both rhodopsin and bacteriorhodopsin, respectively. The driving frequency is fixed to the resonant frequency of rhodopsin (i.e. 1.36 THz), while the damping value is set to 0.3 THz satisfying  $\omega_o > \frac{\gamma}{2}$ . As indicated in the discussion, the presence of such underdamped delocalized modes in proteins has significant implications for the understanding of the efficiency of ligand binding, protein-molecule interactions, as well as biological functions [27]. Moreover, the free energy value,  $\Delta E$ , is set to  $6 k_b T$  since this value is considered as a lower bound for the free energy difference between two states [44].

The folded state of the protein becomes populated when tuning the nanoantenna frequency to the natural vibrational

frequency of the desired protein. This shows that the system gets driven when subjected to the nanoantenna force. For the other untargeted protein, there is a probability that it acquires a folded state if an excessive amount of force is applied to the system. This is why the nanoantenna force should be chosen within a specific window and should not exceed a particular threshold to ensure that it only impacts the protein population of interest. This aspect will be discussed in depth in Sec. V-B3.

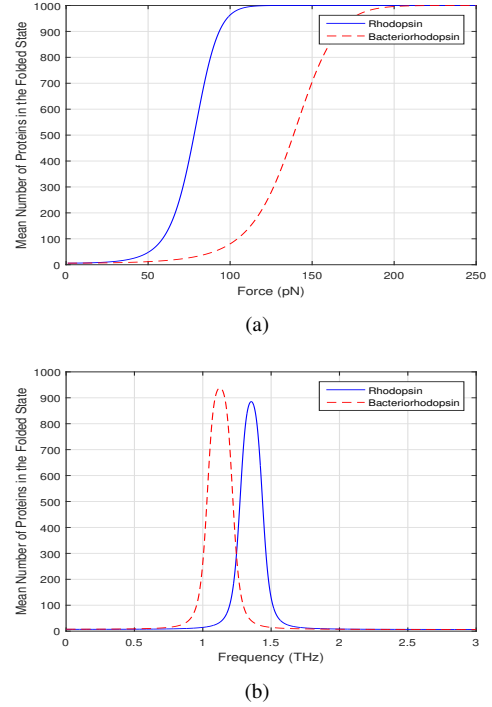


Fig. 1: (a) Mean number of folded proteins versus force. (b) Mean number of folded proteins versus frequency.

Fig. 1b illustrates the expected number of folded proteins versus frequency for both rhodopsin and bacteriorhodopsin. For this case, the value of the nanoantenna force is fixed to 100 pN, while the damping value is set to 0.3 THz. The presented results reveal that by tuning the nanoantenna frequency to the resonant frequency of the protein, the probability of being in a folded state is maximum. As such, the protein can acquire the state which induces the desired biological function. We also observe that the probability of the folded state of bacteriorhodopsin is higher in comparison to rhodopsin since as seen in Table I it has both lower stiffness and mass. This leads to a higher value of the average driving energy,  $\langle E_{tot} \rangle_{ss}$ , indicating that the protein mechanical system plays a role in controlling the protein kinetic rates.

### B. Selectivity of the Nanoantenna-Protein Interaction

1) *Resonant Interactions:* To evaluate the interaction between the nanoantenna and the targeted protein population, we need to compute the selectivity of the system under different scenarios. For all our simulations, we use a force value of  $f_o = 100$  pN and a damping value of  $\gamma = 0.3$  THz. Fig. 2 demonstrates the selectivity versus frequency when

TABLE I: Protein Experimental Values

Protein	Frequency (THz)	Stiffness (N/m)	Mass (kg)	Conformational Change Associated with Vibrational Mode
Rhodopsin	1.36 [41]	3 [42]	$1.62 \times 10^{-24}$	Extracellular loops and helical region near extracellular surface move outward [41].
Bacteriorhodopsin	1.13 [41]	1.9 [42]	$1.48 \times 10^{-24}$	Extracellular loops movement: Helix A (in-out); Helix B (in-out); Helix C (up-down); Helix D (in-out); Helix F (out) [41].
D96N Bacteriorhodopsin	1.025 [41]	Calculated using $\omega_o^2 = k/m$ .	$1.48 \times 10^{-24}$	Entire protein moves in-out of membrane [41].

the targeted protein population is either rhodopsin or bacteriorhodopsin, respectively. We see that, as expected, with equal populations, the interaction achieves maximum selectivity when the nanoantenna is set to the resonant frequency of the desired protein population.

The selectivity value of rhodopsin is 0.9 at 1.36 THz, while that of bacteriorhodopsin is 0.93 at 1.13 THz. The slight difference between the selectivity values of the aforementioned protein populations stems from the fact that the folding probability of bacteriorhodopsin is higher than that of rhodopsin due to its mechanical structure (as explained in Sec. V-A). The presented selectivity results indicate that a high number of proteins of the targeted population has been folded at resonance, with very low false positives. Hence, the THz frequency provides resonant access to protein fundamental modes allowing experimenters to probe molecular responses with high selectivity. The possible outcomes of a nanoantenna-protein interaction are summarized in Table II.

Moreover, at the resonant frequency of the untargeted protein population, a negative selectivity value is attained. As illustrated in Sec. IV, a negative value signifies that the untargeted protein population existing in the system is selected. This acts as a pre-indication for experimenters to avoid getting close to this frequency as it will lead the undesired population to acquire a folded conformation.

Finally, the region of zero crossing in Fig. 2 designates no selectivity. At these frequencies, the mean number of folded proteins of the existing populations is very close to one another, and hence neither population experiences a conformational change.

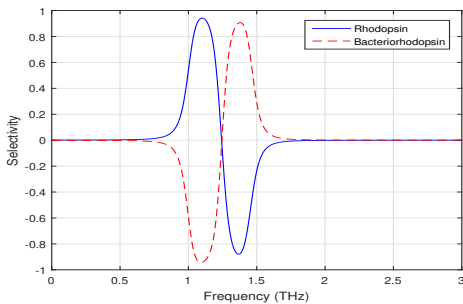


Fig. 2: Selectivity values for the rhodopsin and bacteriorhodopsin population versus frequency.

An important question that arises within this context is how to further achieve a higher selectivity value at resonance. Recall, in our system, a number of parameters act as controlling

factors. Among others, the nanoantenna force plays a fundamental role as its value is determined by the experimenter. Fig. 3 illustrates the selectivity of the rhodopsin population versus the nanoantenna force at its resonant frequency. We see that the nanoantenna force value must be chosen within a specific range to deem the interaction selective. A very low or very high force value will result in zero selectivity since the force will either be too low to fold the protein, or too high making all the proteins in the system fold.

The selected force value depends on several factors including the protein type and system characteristics. For instance, the higher the damping, the more viscous the system is and as such more force is required. Damping provides insights into the dynamics of protein conformational changes by demonstrating the relative significance of frictional forces in activating reactions. Although we cannot control damping as it is dictated by the system, it is beneficial to study its effect on selectivity.

Fig. 4 demonstrates the selectivity of the rhodopsin population versus damping. The force is set to 100 pN and we are still operating at resonance. Similar to the force, damping must be within a certain range for the interaction to be considered selective. The system cannot sustain a high damping value since in this case the viscous forces will impact the capability of identifying the THz modes associated with conformational changes. In other words, the distinct vibrational modes will be faded by the frictional forces and the resonant effect will die out. Nonetheless, this should not be an issue since structured bio-macromolecules such as proteins in the THz frequency range are underdamped, satisfying the condition in which  $\omega_o > \frac{\gamma}{2}$  [27].

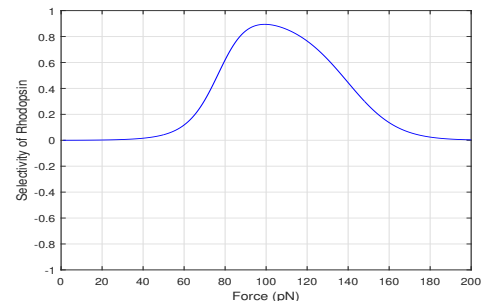
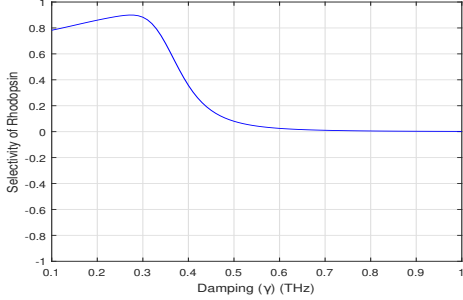


Fig. 3: Selectivity values when targeting the rhodopsin population versus force.

2) *Multiple Proteins*: One important feature of the developed selectivity metric is its applicability to a scenario

TABLE II: Possible Outcomes of a Nanoantenna-Protein Interaction

	Folded Protein State	Unfolded Protein State
Targeted Population	True Positive ( <b>TP</b> )	False Negative ( <b>FN</b> )
Untargeted Population	False Positive ( <b>FP</b> )	True Negative( <b>TN</b> )

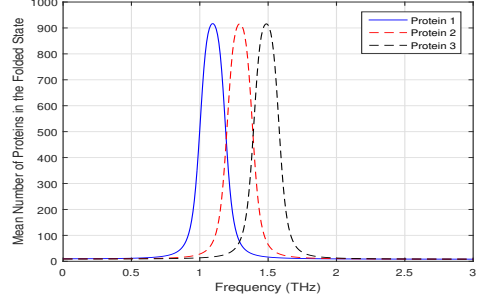
Fig. 4: Selectivity values when targeting the rhodopsin population versus damping,  $\gamma$ .

involving multiple undesired proteins. Such an example fits applications where we are interested in targeting specific disease associated cells amongst others. To illustrate this case, we choose three protein populations with resonant frequencies of 1.1, 1.3 and 1.5 THz, as demonstrated in Fig. 5a. The protein population are of equal abundance,  $n_1 = n_2 = n_3 = 1000$ . We are interested in targeting protein population 2, with a resonant frequency of 1.3 THz.

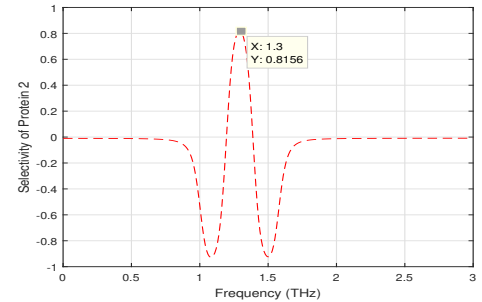
Fig. 5b illustrates selectivity versus frequency. It can be seen that the selectivity is maximum at 1.3 THz, where the marker shows that the selectivity value of protein 2 at resonance is 0.81. Such a high value is an indicator that the desired proteins can be discriminated from the other populations and therefore can be targeted by the nanoantenna. It also confirms the effectiveness of the proposed selectivity metric in capturing the performance of the system.

3) *Joint Optimization*: To design a system that achieves maximum selectivity, we need to know the optimal values of both the nanoantenna force and frequency. Hence, we cast a joint optimization formulation for selectivity with respect to those parameters as explained in Sec. IV-A. Fig. 6 emulates the same scenario provided in Fig. 2. It presents a pseudo-color plot indicating the optimal force and frequency values that must be used when targeting protein rhodopsin in the presence of bacteriorhodopsin. The color map demonstrates the intensity of the selectivity value. Similarly, Fig. 7 presents a pseudo-color plot, which mimics the scenario presented in Fig. 5. It also provides the force and frequency values that result in obtaining a maximum selectivity when targeting protein population 2 in the presence of populations 1 and 3.

We can notice from Figs. 6 and 7 that the joint optimization is a very powerful tool that provides experimenters with access to the optimal force and frequency values. As such, they can guarantee that the system achieves maximum selectivity and that the targeted protein population acquires the desired folding behavior. The color map provides a visualization of the number of protein populations considered in each system



(a)



(b)

Fig. 5: (a) Mean number of folded proteins versus frequency for protein population 1, 2 and 3. (b) Selectivity values for protein 2 population versus frequency.

and it clearly discriminates regions that should be targeted from those that should be avoided in order not to activate the wrong proteins.

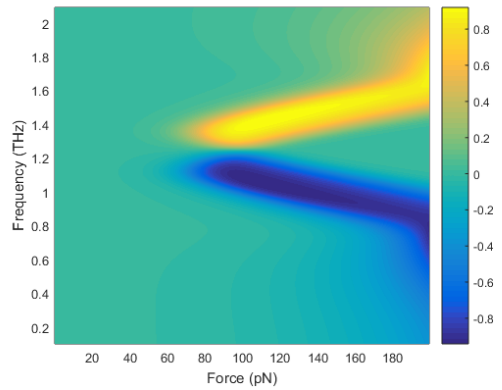


Fig. 6: Pseudo-color plot showing the optimal force and frequency for targeting rhodopsin in the presence of bacteriorhodopsin.

4) *Shift in Optimal Frequency*: In Fig. 2, we noticed that a maximum selectivity is always achieved at resonance. This

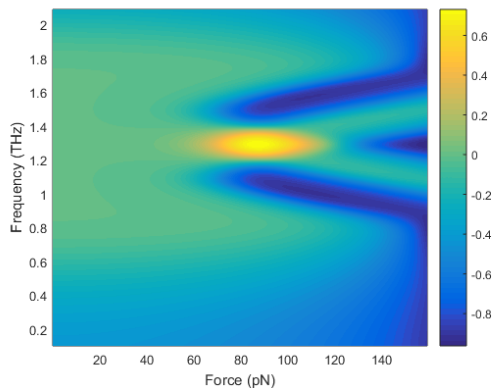


Fig. 7: Pseudo-color plot showing the optimal force and frequency for targeting protein population 2 ( $\omega = 1.3$  THz) in the presence of population 1 ( $\omega = 1.1$  THz) and population 3 ( $\omega = 1.5$  THz).

occurs when the resonant frequency difference between the proteins involved is within a certain range. In fact, if the difference between the protein resonant frequencies is  $\geq 0.2$  THz, then selectivity is always maximum at resonance. This value has been attained after conducting several simulation trials and experimenting with different proteins of varying resonances. Nevertheless, if the difference is less than 0.2 THz, the overlap between the protein populations gets larger and more of the untargeted protein population gets folded resulting in a higher number of false positives. Such an impact not only lowers the selectivity value but also affects the frequency at which the maximum response is achieved.

Fig. 8a presents the mean number of folded proteins for two protein populations with close resonant frequencies and equal abundance, namely, bacteriorhodopsin ( $\omega = 1.3$  THz) and D96N bacteriorhodopsin. The latter is a bacteriorhodopsin mutant with a resonant frequency of 1.025 THz [41]. The difference in their resonant frequency is  $\approx 0.1$  THz. This results in a higher overlap between the protein populations.

Fig. 8b shows the selectivity of bacteriorhodopsin versus frequency in the presence of the D96N mutant. It can be seen that not only has the selectivity value decreased to  $\approx 0.78$  in comparison to the selectivity of bacteriorhodopsin in Fig. 2, but the maximum selectivity is achieved at 1.17 THz rather than the expected resonant frequency of 1.13 THz. Thereby, the selectivity metric is important since it indicates the frequency at which the maximum system desired response is achieved; this could be at the resonant frequency,  $\omega_o$ , or at a frequency close to it.

If we considered an imbalance in population, in which for example  $n_1 = 800$  proteins, while  $n_2 = 1000$  proteins, the selectivity value is going to decrease. This occurs since the number of proteins of the targeted population has decreased, resulting in a lower number of folded proteins. The counter-effect occurs if the number of proteins in the targeted population is larger than the untargeted one, where the selectivity value is going to increase.

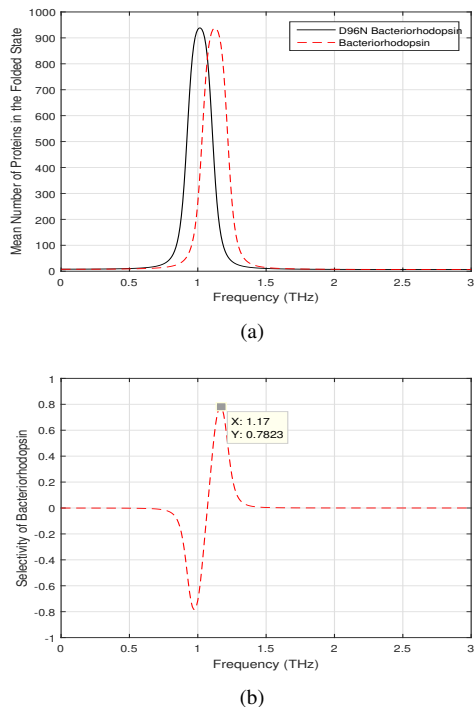


Fig. 8: (a) Mean number of folded proteins versus frequency for bacteriorhodopsin and D96N bacteriorhodopsin. (b) Selectivity values for bacteriorhodopsin population versus frequency.

## VI. CONCLUSIONS

In this paper, we derive an expression for the selectivity of the nanoantenna-protein response. Selectivity serves as a metric that allows us to study whether the interaction between the nanoantenna and the protein is sufficient to provoke a conformational change in the desired protein molecule/population in the presence of other proteins. The metric provides a score that ranges between  $-1$  and  $1$ . A value of  $-1$  indicates the worst-case scenario, where only the undesired protein molecule/population is being provoked to fold. On the contrary, a value of  $1$  indicates the best-case scenario, where only the desired protein molecule/population is being stimulated to fold. As such, the closer the value achieved to is  $1$ , the higher the selectivity in the system. According to the selectivity values attained, an experimenter can determine the level of control over the desired nanoantenna-protein interaction. The effectiveness of the proposed metric is seen from the different tested scenarios.

To develop the selectivity metric, we deploy the Langevin stochastic equation driven by an external force to capture the protein dynamics in an intra-body environment. We then formulate an expression for the steady-state energy stimulating the protein to change its conformation and use it to amend Boltzmann distribution. For the numerical analysis, we consider well-studied proteins with experimental parameters available in the literature. The achieved results provide an understanding of the impact of the system parameters, namely, the nanoantenna force, damping, and protein abundance on the

performance. Such analysis provides genuine insight into the conditions at which maximum selectivity is achieved.

The presented work provides a novel perspective regarding signal transduction processes, where proteins are controlled via EM waves to obtain their functional conformation as part of a vibratory network. By understanding how THz waves may alter the pathological mechanisms in intra-body networks, the development of therapeutic strategies shall be enabled and wide-scale shift by pharmaceutical research is motivated.

## REFERENCES

- [1] R. M. Shubair and H. Elayan, "In vivo wireless body communications: State-of-the-art and future directions," in *2015 Loughborough Antennas & Propagation Conference (LAPC)*. IEEE, 2015, pp. 1–5.
- [2] K. Yang *et al.*, "Numerical analysis and characterization of THz propagation channel for body-centric nano-communications," *IEEE Transactions on Terahertz Science and Technology*, vol. 5, no. 3, pp. 419–426, May 2015.
- [3] Q. H. Abbasi *et al.*, "Terahertz channel characterization inside the human skin for nano-scale body-centric networks," *IEEE Transactions on Terahertz Science and Technology*, vol. 6, no. 3, pp. 427–434, 2016.
- [4] H. Elayan, R. M. Shubair, J. M. Jornet, and P. Johari, "Terahertz channel model and link budget analysis for intrabody nanoscale communication," *IEEE Transactions on Nanobioscience*, vol. 16, no. 6, pp. 491–503, 2017.
- [5] H. Elayan, R. M. Shubair, J. M. Jornet, and R. Mittra, "Multi-layer intrabody terahertz wave propagation model for nanobiosensing applications," *Nano Communication Networks*, vol. 14, pp. 9–15, 2017.
- [6] L. Wei *et al.*, "Application of terahertz spectroscopy in biomolecule detection," *Frontiers in Laboratory Medicine*, vol. 2, no. 4, pp. 127–133, 2018.
- [7] A. G. Markelz, "Terahertz dielectric sensitivity to biomolecular structure and function," *IEEE Journal of Selected Topics in Quantum Electronics*, vol. 14, no. 1, pp. 180–190, 2008.
- [8] G. Acbas *et al.*, "Optical measurements of long-range protein vibrations," *Nature communications*, vol. 5, no. 1, pp. 1–7, 2014.
- [9] A. Carpinteri *et al.*, "Terahertz mechanical vibrations in lysozyme: Raman spectroscopy vs modal analysis," *Journal of Molecular Structure*, vol. 1139, pp. 222–230, 2017.
- [10] A. Carpinteri, G. Piana, A. Bassani, and G. Lacidogna, "Terahertz vibration modes in Na/K-ATPase," *Journal of Biomolecular Structure and Dynamics*, vol. 37, no. 1, pp. 256–264, 2019.
- [11] H. Elayan, A. Eckford, and R. Adve, "Regulating Molecular Interactions Using Terahertz Communication," in *IEEE International Conference on Communications (ICC)*. IEEE, 2020, pp. 1–6.
- [12] H. Elayan, A. W. Eckford, and R. S. Adve, "Information rates of controlled protein interactions using terahertz communication," *IEEE Transactions on NanoBioscience*, vol. 20, no. 1, pp. 9–19, 2020.
- [13] E. R. Beyerle and M. G. Guenza, "Kinetics analysis of ubiquitin local fluctuations with Markov state modeling of the LE4PD normal modes," *The Journal of chemical physics*, vol. 151, no. 16, p. 164119, 2019.
- [14] V. Aglieri *et al.*, "Improving nanoscale terahertz field localization by means of sharply tapered resonant nanoantennas," *Nanophotonics*, vol. 9, no. 3, pp. 683–690, 2020.
- [15] M. Rahm *et al.*, "Focus on terahertz plasmonics," *New Journal of Physics*, vol. 17, no. 10, p. 100201, 2015.
- [16] E. Manikandan, S. Princy, B. Sreeja, and S. Radha, "Structure metallic surface for terahertz plasmonics," *Plasmonics*, vol. 14, no. 6, pp. 1311–1319, 2019.
- [17] D. M. Mittleman, "Frontiers in terahertz sources and plasmonics," *Nature Photonics*, vol. 7, no. 9, pp. 666–669, 2013.
- [18] X. Zhang *et al.*, "Terahertz surface plasmonic waves: a review," *Advanced Photonics*, vol. 2, no. 1, p. 014001, 2020.
- [19] S. Romanenko *et al.*, "The interaction between electromagnetic fields at megahertz, gigahertz and terahertz frequencies with cells, tissues and organisms: risks and potential," *Journal of The Royal Society Interface*, vol. 14, no. 137, p. 20170585, 2017.
- [20] J. Knab, J.-Y. Chen, and A. Markelz, "Hydration dependence of conformational dielectric relaxation of lysozyme," *Biophysical journal*, vol. 90, no. 7, pp. 2576–2581, 2006.
- [21] A. Bassani, "Terahertz Vibrations in Proteins: Experimental and Numerical Investigation," Ph.D. dissertation, Politecnico di Torino, 2017.
- [22] K.-C. Chou and N.-Y. Chen, "The biological functions of low-frequency phonons," *Scientia Sinica*, vol. 20, no. 4, pp. 447–457, 1977.
- [23] W. Nadler, A. T. Brünger, K. Schulten, and M. Karplus, "Molecular and stochastic dynamics of proteins," *Proceedings of the National Academy of Sciences*, vol. 84, no. 22, pp. 7933–7937, 1987.
- [24] S. S. Seyedi and D. V. Matyushov, "Protein dielectrophoresis in solution," *The Journal of Physical Chemistry B*, vol. 122, no. 39, pp. 9119–9127, 2018.
- [25] V. Balakrishnan, *Elements of nonequilibrium statistical mechanics*. Ane Books, 2008, vol. 3.
- [26] F. W. Byron and R. W. Fuller, *Mathematics of classical and quantum physics*. Courier Corporation, 2012.
- [27] D. A. Turton *et al.*, "Terahertz underdamped vibrational motion governs protein-ligand binding in solution," *Nature communications*, vol. 5, no. 1, pp. 1–6, 2014.
- [28] D. Liu, X.-q. Chu, M. Lagi, Y. Zhang, E. Fratini, P. Baglioni, A. Alatas, A. Said, E. Alp, and S.-H. Chen, "Studies of phononlike low-energy excitations of protein molecules by inelastic x-ray scattering," *Physical review letters*, vol. 101, no. 13, p. 135501, 2008.
- [29] Y. Deng *et al.*, "Near-field stationary sample terahertz spectroscopic polarimetry for biomolecular structural dynamics determination," *ACS Photonics*, vol. 8, no. 2, pp. 658–668, 2021.
- [30] M. Yaghoubi, M. E. Fouladvand, A. Bérut, and J. Łuczka, "Energetics of a driven Brownian harmonic oscillator," *Journal of Statistical Mechanics: Theory and Experiment*, vol. 2017, no. 11, p. 113206, 2017.
- [31] I. Y. Orhan and B. A. Gulbahar, "Stimulation of protein expression through the harmonic resonance of frequency-specific music," *Clinical and Investigative Medicine*, pp. S34–S38, 2016.
- [32] H. Elayan, A. W. Eckford, and R. Adve, "Enabling Protein Interactions Using Terahertz Signals for Intra-body Communication," in *Proceedings of the 19th ACM Conference on Embedded Networked Sensor Systems*, 2021, pp. 603–609.
- [33] A. W. Orr, B. P. Helmke, B. R. Blackman, and M. A. Schwartz, "Mechanisms of mechanotransduction," *Developmental cell*, vol. 10, no. 1, pp. 11–20, 2006.
- [34] A. V. Finkelstein *et al.*, "Why do protein architectures have Boltzmann-like statistics?" *Proteins: Structure, Function, and Bioinformatics*, vol. 23, no. 2, pp. 142–150, 1995.
- [35] F. Sachs and H. Lecar, "Stochastic models for mechanical transduction," *Biophysical journal*, vol. 59, no. 5, pp. 1143–1145, 1991.
- [36] C. B. Anfinsen, "Principles that govern the folding of protein chains," *Science*, vol. 181, no. 4096, pp. 223–230, 1973.
- [37] P. Sweeney *et al.*, "Protein misfolding in neurodegenerative diseases: implications and strategies," *Translational neurodegeneration*, vol. 6, no. 1, pp. 1–13, 2017.
- [38] N. Bosc, C. Meyer, and P. Bonnet, "The use of novel selectivity metrics in kinase research," *BMC bioinformatics*, vol. 18, no. 1, pp. 1–12, 2017.
- [39] D. L. Bostick and C. L. Brooks, "Selectivity in K<sup>+</sup> channels is due to topological control of the permeant ion's coordinated state," *Proceedings of the National Academy of Sciences*, vol. 104, no. 22, pp. 9260–9265, 2007.
- [40] A. Cegielski, *Iterative methods for fixed point problems in Hilbert spaces*. Springer, 2012, vol. 2057.
- [41] R. Balu *et al.*, "Terahertz spectroscopy of bacteriorhodopsin and rhodopsin: similarities and differences," *Biophysical journal*, vol. 94, no. 8, pp. 3217–3226, 2008.
- [42] K. T. Sapra, P. S.-H. Park, K. Palczewski, and D. J. Muller, "Mechanical Properties of Bovine Rhodopsin and Bacteriorhodopsin: Possible Roles in Folding and Function," *Langmuir*, vol. 24, no. 4, pp. 1330–1337, 2008.
- [43] A. D. MacKerell Jr *et al.*, "All-atom empirical potential for molecular modeling and dynamics studies of proteins," *The journal of physical chemistry B*, vol. 102, no. 18, pp. 3586–3616, 1998.
- [44] C. J. Benham *et al.*, *Mathematics of DNA structure, function and interactions*. Springer Science & Business Media, 2009, vol. 150.